J Electroceram (2006) 17:87–90
DOI 10.1007/s10832-006-9943-8

Fabrication and characterization of Fe_3O_4/CNTs and Fe_2N/CNTs composites

Linqin Jiang · Lian Gao

Abstract By controlling the nitridation temperature, magnetic nanoparticles (Fe_3O_4 and Fe_2N) were attached to the carbon nanotubes (CNTs) to fabricate new Fe_3O_4/CNTs and Fe_2N/CNTs composites with magnetic property from the same precursor. The attachment of tiny magnetic nanoparticles on CNTs is crucial for the formation of a homogeneous composite, which provides good combination between CNTs and the magnetic matrix to give a CNT-combined composite. Both Fe_3O_4/CNTs and Fe_2N/CNTs composites show magnetic characteristic from the hysteresis loops measurements at room temperature. Morever, these composites have greater specific surface areas than pure Fe_3O_4 and Fe_2N materials, which means that these composites are promising as good adsorbents for removal of contaminants from water and easily seperated from the medium by a magnetic process.

Keywords Carbon nanotubes · Magnetite · Iron nitride · Magnetic property

Introduction

Since the bulk production of CNTs has become possible and practical, there is growing interest in the fabrication and property characterization of CNT-combined composites [1–3]. The development of CNT-incorporated advanced engineering composites has become an attractive concept due to their excellent magnetic, thermal and electrical properties [4, 5]. Morever, because CNTs can be thought of as cylindrical hollow micro-crystals of graphite and have a relatively large specific surface area, they have attracted researchers' interest as a new type of support and offer an attractive option for the removal of organic and inorganic contaminants from water [6–8].

The application of magnetic particle technology to solve environmental problems has received considerable attention in recent years. Magnetic particles can be used to adsorb contaminants from aqueous or gaseous effluents and, after adsorption, can be separated from the medium by a simple magnetic process [9]. Peng et al. [6] reported Fe_3O_4/γ-Fe_2O_3/CNTs magnetic composites can be used to adsorb contaminants from aqueous effluents and after the desorption is carried out, the adsorbent can be separated from the medium by a magnetic process. Our previous work has synthesized Fe_3O_4/CNTs composite by solvothermal method [10].

In this work, new magnetic nanoparticles-attached CNTs composites (Fe_3O_4/CNTs and Fe_2N/CNTs) were prepared by nitriding the same precursor at different temperature. The composites show higher specific surface area compared to pure materials without CNTs and retain the magnetic properties.

Experimental section

CNTs prepared by the catalytic decomposition of CH_4 were kindly provided by Shenzhen Nanoport company. The microstructure of CNTs was observed in our previous work [10]. Pristine CNTs were oxidized by refluxing at 140°C in concentrated nitric acid for 24 h. The acid-refluxed CNTs can not only provide good combination with magnetic nanoparticles due to the functional groups on the nanotubes but also be good adsorbents for pollutants in water [6].

L. Jiang · L. Gao (✉)
State Key Laboratory of High Performance Ceramics and Superfine Microstructure, Shanghai Institute of Ceramics, Chinese Academy of Sciences, 1295 Ding Xi Road, Shanghai 200050
e-mail: liangaoc@online.sh.cn

L. Jiang
Graduate School of the Chinese Academy of Sciences, P.R. China

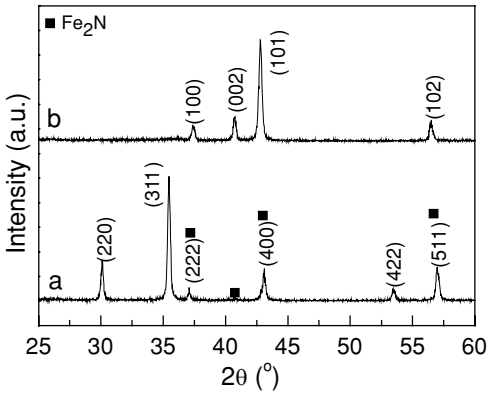

Fig. 1 XRD patterns of: (a) Fe_3O_4/CNTs composite nitrided at 400°C for 4 h in an NH_3 atmosphere and (b) Fe_2N/CNTs composite nitrided at 500°C for 4 h in an NH_3 atmosphere

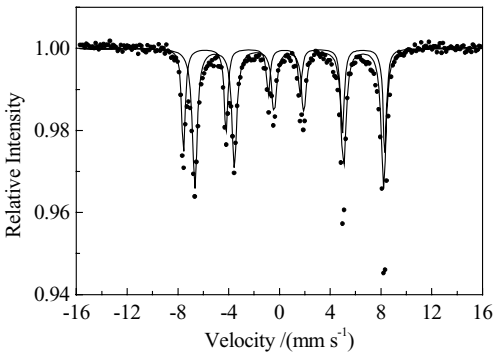

Fig. 2 Mössbauer spectrum of the Fe_3O_4/CNTs composite powders measured at room temperature

Iron nitrate [$Fe(NO_3)_3 \cdot 9H_2O$], used as a starting material, was dissolved in aquous solution to form 54 ml of 0.6 M solution. Then 0.2 g acid-treated MWNTs was added into the solution and then the suspension was ultrasonicated for 5 min 2.5 M ammonia solution was dropwised into the above mixed solution with vigorous stirring until the final pH of the suspension reached above 9. The precipitate was filtered, rinsed with anhydrous ethanol, and then dried at 80°C for 24 h. The sample was subsequently calcinated at 300°C for 2 h. The obtained powders were loaded into a quartz boat and heated in flowing NH_3 (1 L min^{-1}) at 400 and 500°C for 4 h in a tube furnace to obtain Fe_3O_4/CNTs and Fe_2N/CNTs composites, respectively. The same method was applied to fabricate pure Fe_3O_4 and Fe_2N powders without CNTs.

The X-ray diffraction patterns of the synthesized composites were obtained by powder X-ray diffraction (XRD, D/Max 2550V, Rigaku, Japan), using Cu K_α radiation ($\lambda = 1.5418$ Å). Mössbauer spectroscopic study (MS, Series 40 MCA, Canberra, USA) for the obtained composite was performed using a source of ^{57}Co in a Pd matrix at room temperature. The specific surface areas of the powders were measured by nitrogen adsorption using a surface area analyzer (ASAP 2010, Micrometrices, USA). Transmission electron microscopy (TEM, JEM 2010, JEOL, Japan) was performed to observe the microstructure of the composite. Energy-dispersive spectrocopy (EDS) was also taken on the same apparatus. Magnetic measurements at room temperature were carried out on a Lake Shore 7400 vibrating sample magnetometer (VSM).

Results and discussion

The CNT-based composites obtained after nitridation were determined using XRD, as shown in Fig. 1. The XRD peaks (curve a) correspond with the reported values of Fe_3O_4 (JCPDS 19-0629) and Fe_2N (JCPDS 02-1206) in curve a and b, respectively. The sample in curve a also contains a little Fe_2N. Reduction at 400°C in NH_3 atmosphere in the presence of CNTs may give rise to extensive production of a little Fe_2N. According to the XRD patterns, the lattice parameter a of cubic phase for Fe_3O_4/CNT composite was calculated by the relation: $d_{h^*k^*l^*} = \frac{a}{\sqrt{h^{*2}+k^{*2}+l^{*2}}}$ using the (311) peak. Thus, the value of a is 8.389, which is close to the standard value (8.396) in JCPDS 19-0629. For Fe_2N/CNT composite, the lattice parameters (a and c) of hexagonal phase were calculated by the relation: $\sin^2\theta = a(h^2 + hk + k^2) + cl^2$, where $A = \lambda^2/3a^2$ and $C = \lambda^2/4c^2$ using the (100) and (101) peaks. The values of a and c are 2.776 and 4.418, respectively, which are close to the standard value ($a = 2.755$ and $c = 4.410$) in JCPDS 02-1206.

Though the XRD patterns of Fe_3O_4 are similar to those of γ-Fe_2O_3, there are still slight differences between them [11]. In curve a in Fig. 1, the peaks can be well indexed with Fe_3O_4 reflection. The black color of the samples suggests the formation of Fe_3O_4. The Mössbauer spectrum (as shown in Fig. 2) consists of two hyperfine magnetic sextets, one for Fe^{3+} at tetrahedral sites and the other for the mixed valence $Fe^{2.5+}$ at octahedral sites. This result also indicates that the product is Fe_3O_4 [12].

The morphologies of the Fe_3O_4/CNT and Fe_2N/CNT composites were examined by TEM and HRTEM, as shown in Figs. 3 and 4, respectively. For both of the composites, the typical micrographs in Figs. 3(a) and 4(a) clearly show that tiny nanoparticles are well attached to the CNTs, with a diameter of 10∼20 nm. To investigate the composition of these nanoparticles, EDS measurements were performed. The EDS spectra (shown in the inset of Figs. 3(a) and 4(a)) indicate these tiny particles anchored on the nanotube consist of Fe_3O_4 and Fe_2N, respectively. The Fe_3O_4/CNT composite also shows small N peak in EDS spectrum, which corresponds with the XRD result. The lattice fringe spacing of the attached nanocrystal are indexed as the (222) or (311) plane of the Fe_3O_4 reflection in Fig. 3(b) and the (101) or (100) plane of the Fe_2N reflection in Fig. 4(b), respectively.

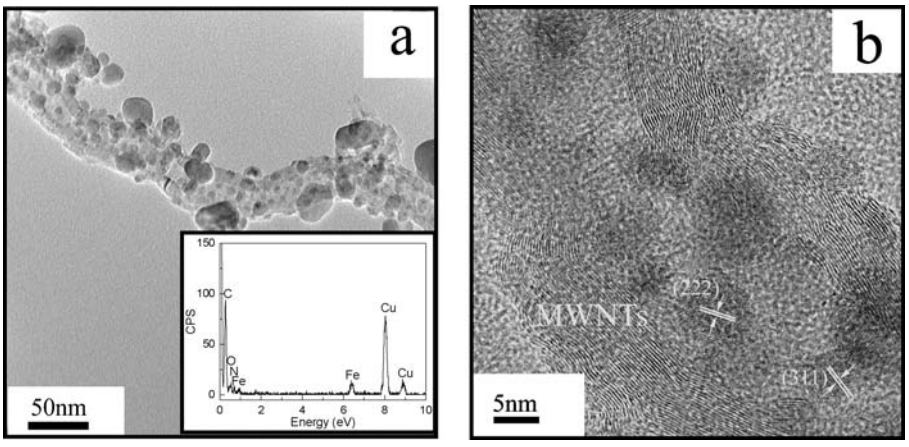

Fig. 3 TEM and HRTEM image of the Fe_3O_4/CNTs composite. The EDS spectrum of the attached nanoparticles on CNTs is shown in the inset of (a)

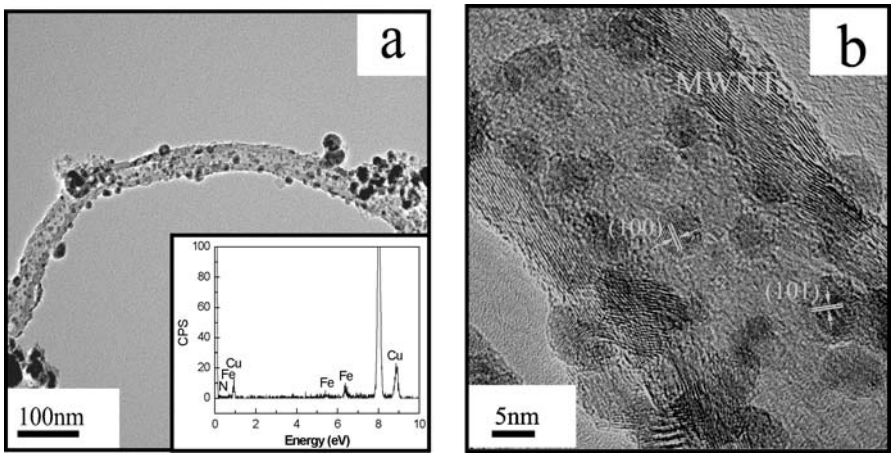

Fig. 4 TEM and HRTEM image of Fe_2N/CNTs composite. The EDS spectrum of the attached nanoparticles on CNTs is shown in the inset of (a)

In this work, the acidic functional groups were introduced on the CNTs surface by the reflux and greatly altered their surface charge properties. These functional groups exist on the surface of the tubes and make them easily dispersed in polar solvents, such as water, ethanol, etc. [13]. In the course of attaching CNTs with magnetic nanoparticles, the functional groups introduced by surface oxidation play an important role. Due to the electrostatic attraction, the Fe^{3+} ions adsorb onto the surface of the acid treated CNTs [14]. Then, upon further addition of OH^-, the metal ions in situ react with them, and FeOOH precursors are formed as coatings on the CNTs surface. After calcination and nitridation, tiny magnetic particles were produced *in situ* on the CNTs. In addition, because of the restriction effect of CNTs on the growth of attached particles [15], the diameter of the magnetic nanoparticles attached on the nanotubes is only about 10∼20 nm, much smaller than bulk particles which are mostly in the range of ca. 80∼100 nm (not shown) .

According to the results of XRD and EDS, the Fe_3O_4/CNT and Fe_2N/CNT composites can be obtained at different temperature in NH_3 atmosphere from the same precursor of FeOOH/CNT powders. The NH_3 decomposes into molecular N_2 and H_2 at temperatures above 200–300°C [16]. For Fe_3O_4/CNT composite, the H_2 can be used as a reductive atmosphere to reduce Fe_2O_3 to Fe_3O_4 and a little Fe_2N, which can be seen from XRD and EDS results. Further elevating the nitridation temperature to 500°C makes the precursor fully nitride into Fe_2N.

Since the application of magnetic particle technology to solve environmental problems requires the magnetic material has a high surface area of a high absorption capacity [9], BET measurment was applied to these composites. It is well known that the acid-treated CNTs has great specific surface area (199.4 $m^2 \cdot g^{-1}$), and therefore is expected to increase the surface area of the CNT-based composites [6]. From the BET results, it is found that the surface area (S_{BET}) of the composites is greatly increased in the presence of CNTs. The S_{BET} of pure Fe_3O_4 and Fe_2N is only 15.77 and 10.67 $m^2\ g^{-1}$, respectively. After the addition of 5 wt% CNTs, the S_{BET} of Fe_3O_4/CNT and Fe_2N/CNT composites are increased to 30.65 and 26.24 $m^2\ g^{-1}$ by 1.9 and 2.4 times, respectively. It can be suggested that CNTs can effectively enhance the

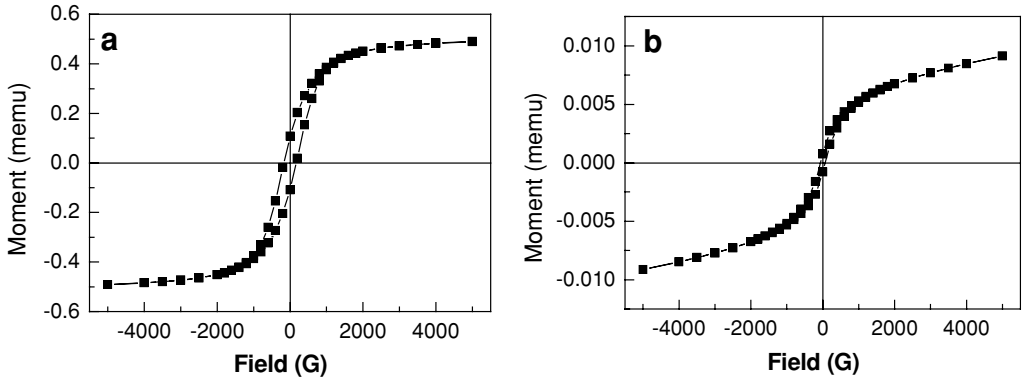

Fig. 5 Magnetic hysteresis curves for: (a) Fe_3O_4/CNTs and (b) Fe_2N/CNTs composites measured at room temperature

surface area of the CNT-based composites, which is promising for good adsorbents for the removal of organic and inorganic contaminants from water.

The magnetic properties for Fe_3O_4/CNTs and Fe_2N/CNTs composites are shown in Fig. 5. The saturation magnetization of Fe_3O_4/CNTs composite is higher than that of Fe_2N/CNTs material. After the addition of CNTs, these composites still has magnetic properties. It can be foreseen that these composites would be potential in the application of absorbants for the removal of contamitants from water because the adsorbents can be easily separated from the medium by a magnetic process after the adsorption is carried out.

Conclusions

New Fe_3O_4/CNTs and Fe_2N/CNTs magnetic composites were successfully fabricated. In the presence of CNTs, the Fe_3O_4/CNT and Fe_2N/CNT composites exhibit 1.9 and 2.4 times enhancement in the specific surface area over that of pure Fe_3O_4 and Fe_2N material, respectively. The fabrication of tiny magnetic nanoparticles attached on individual CNTs facilitates interfacial adhesion between the CNTs and the magnetic matrix. The Fe_3O_4/CNTs and Fe_2N/CNTs magnetic composites containing tiny magnetic nanoparticle-attached nanotube with increased surface area have great promise as an effective adsorbants for removal contaminants from aqueous effluents.

Acknowledgment Authors thank for the support from National Nature Science Foundation of China (No. 50372077).

References

1. J. Sandler, M.S.P. Shaffer, T. Prasse, W. Bauhofer, K. Schulte, and A.H. Windle, *Polymer*, **40**, 5967 (1999).
2. A. Peigney, Ch. Laurent, and A. Rousset, *Key. Eng. Mater*, **743**, 132 (1997).
3. E. Flahaut, A. Peigney, Ch. Laurrent, Ch, Marlière, F. Chastel, and A. Rousset, *Acta. Mater*, **48**, 3803 (2000).
4. W.A. Heer, A. Chatelain, and D.A. Ugarte, *Science*, **270**, 1179 (1995).
5. R.F. Service, *Science*, **271**, 1232 (1996).
6. X.J. Peng, Z.K. Luan, Z.C. Di, Z.G. Zhang, and C.L. Zhu, *Carbon*, **43**, 855 (2005).
7. Y.H. Li, S. Wang, A. Cao, D. Zhao, X. Zhang, C. Xu, Z. Luan, D. Ruan, J. Liang, D. Wu, and B. Wei, *Chem. Phys. Lett.*, **350**, 412 (2001).
8. X. Peng, J. Ding, Z. Di, Y. Li, Z. Luan, and B. Tian, *Mater. Lett.*, **59**, 399 (2005).
9. L.C.A. Oliveira, R.V.R.A. Rios, J.D. Fabris, V. Garg, K. Sapag, and R.M. Lago, *Carbon*, **40**, 2177 (2002).
10. L.Q. Jiang and L. Gao, *Chem. Mater.*, **15**, 2848 (2003).
11. D. Chen and R. Xu, *Mater. Res. Bull.*, **33**, 1015 (1998).
12. R. Bauminger, S.G. Cohen, A. Marinov, S. Ofer, and E. Segal, *Phys. Rev*., **122**, 1447 (1961).
13. J. Liu, A.G. Rinzler, H.J. Dai, J.H. Hafner, K. Bradley, and P.J. Boul, *Science*, **280**, 1253 (1998).
14. Y.Q. Liu and L. Gao, *Carbon*, **43**, 47 (2005).
15. L.Q. Jiang and L. Gao, *J. Mater. Chem*., **15**, 260 (2005).
16. Y. Qiu and L. Gao, *J. Euro. Ceram. Soc*., **23**, 2015 (2003).